Predictive Control Based Speed, Torque and Flux Prediction of a Double Stator Induction Motor

Houari Khouidmi[1*], Ahmed Massoum[2]
1- Hassiba Benbouali University of Chlef. Po.Box 151 Hay Es-Salem Chlef 02000-Algeria.
Email: h.khouidmi@univhb-chlef.dz (Corresponding author)
2- Djillali Liabès University of Sidi Bel-Abbès. P.o. Box 89 Sidi Bel-abbès, 22000- Algeria.
Email: amassoum@univ-sba.dz

Received: December 2017 Revised: March 2018 Accepted: June 2018

ABSTRACT:
The predictive control based speed, flux and torque prediction of a double stator induction motor is proposed in this research paper; the model of the DSIM and the direct vector control of the system have performed, subsequently, the classical PI controllers for the speed control, the flux, and thus for setting the stator's currents have adopted. In order to minimize the transient control and to reduce the impact of measurement noise on the control signal, instead of vector control technique which requires the flux and torque estimation, the multivariable generalized predictive control is used. The results have shown the effectiveness of the proposed method, especially in the parameters variation and/or the change of the reference speed.

KEYWORDS: Double Stator Induction Motor, Direct Field Oriented Control, Predictive Control.

1. INTRODUCTION

The dual star induction machine (DSIM) or double stator induction machine has been the subject of numerous studies for a long time. It has the advantage of being robust, reliable and poorly functioning in degraded operation. Unfortunately, it has a major disadvantage, its dynamic structure is highly nonlinear and the internal variables such as the electromagnetic torque and the rotor flux are strongly coupled, which makes the control of this machine complex [1-3].

Indeed, the vector control makes it possible to envisage a decoupling between the electromagnetic torque and the rotor flux of the machine and to achieve a control comparable to that of the dc machines [4]. This method of control was carried out in 1971 and 1972 by HASS and BLASCHKE [5]. Several similar techniques, but with some differences in the interpretation of key concepts, have been proposed in the field of induction machine control [6], [7]. For example, scalar control, direct torque control, input/output linearization control, etc. Most of these techniques are based on linear modeling of the machine. For the reason of facilitation processing, the case of a linear model also has the advantage of being situated in a very rich theoretical context [8].

The generalized predictive control proves a sufficiently complete structure proposed to solve a very general problem, providing a stable system for a set of adjustment parameters [9], [10,]. This strategy allows to control processes with non-minimal phase shift, with unstable or poorly damped poles, with dead times, constant or unknown, or with an unknown order model. It has proven its efficiency, flexibility and success in industrial applications [11].

The main contribution of this paper is the implementation of a high-performance predictive control law for a double stator induction motor, with as objectives: improve the pursuit of trajectories, guarantee the stability, the robustness to the variations of the parameters and disturbance rejection. This control strategy is used to develop a multivariable predictive control technique based on the prediction of the electromagnetic torque and the rotor flux to generate the switching states of the inverter and consequently the supply voltages of the DSIM.

The paper is organized as follows: the double stator induction motor (DSIM) model and the vector control strategy are presented in section 2 and 3 respectively. In Section 4 the multivariable predictive control strategies are discussed. In section 5 and 6 the application of the resulting predictive control of DSIM is provided. Finally, the overall proposed predictive control scheme of DSIM shown in Fig.1 is used for numerical simulation and the related results and remarks are presented.

2. DSIM MODEL

The Orthogonal subspaces α-β model of the double stator induction machine is presented in Fig 2. The equations of this machine can be expressed in (α, β) axes where the attributed reference is the stator field [3], [4].

1.1. Voltages Equations

By choosing a referential related to the stator field, we obtain the following system of equations [1-4]:

$$\begin{cases} v_{s\alpha1} = R_{s1} i_{s\alpha1} + \dfrac{d\Phi_{s\alpha1}}{dt} \\ v_{s\beta1} = R_{s1} i_{sq1} + \dfrac{d\Phi_{s\beta1}}{dt} \\ v_{s\alpha2} = R_{s2} i_{s\alpha2} + \dfrac{d\Phi_{s\alpha2}}{dt} \\ v_{s\beta2} = R_{s2} i_{s\beta2} + \dfrac{d\Phi_{s\beta2}}{dt} \\ 0 = R_r i_{r\alpha} + \dfrac{d\Phi_{r\alpha}}{dt} + \omega_r \Phi_{r\beta} \\ 0 = R_r i_{r\beta} + \dfrac{d\Phi_{r\beta}}{dt} + \omega_r \Phi_{r\alpha} \end{cases} \quad (1)$$

Where:

$v_{s1\alpha\beta}$ $v_{s2\alpha\beta}$	:First and second stator voltages in stationary frame
$i_{s1\alpha\beta}$ $i_{s2\alpha\beta}$	:First and second stator currents in the stationary frame
$\Phi_{s1\alpha\beta}$ $\Phi_{s2\alpha\beta}$	:First and second stator flux in the stationary frame
$\Phi_{r\alpha\beta}$	:Rotor flux in stationary frame
ω_r	:Rotor frequency
R_{s12} R_r	:First and second stator and rotor resistance

1.2. Flux Equations

The relations between flux and currents are given by [1-4]:

$$\begin{cases} \Phi_{s\alpha1} = L_{s1} i_{s\alpha1} + L_m (i_{s\alpha1} + i_{s\alpha2} + i_{r\alpha}) \\ \Phi_{s\beta1} = L_{s1} i_{s\beta1} + L_m (i_{s\beta1} + i_{s\beta2} + i_{r\beta}) \\ \Phi_{s\alpha2} = L_{s2} i_{s\alpha2} + L_m (i_{s\alpha1} + i_{s\alpha2} + i_{r\alpha}) \\ \Phi_{s\beta2} = L_{s2} i_{s\beta2} + L_m (i_{s\beta1} + i_{s\beta2} + i_{r\beta}) \\ \Phi_{r\alpha} = L_r i_{r\alpha} + L_m (i_{s\alpha1} + i_{s\alpha2} + i_{r\alpha}) \\ \Phi_{r\beta} = L_r i_{r\beta} + L_m (i_{s\beta1} + i_{s\beta2} + i_{r\beta}) \end{cases} \quad (2)$$

Where:

L_{s12}	:First and second stator inductance
L_r	:Rotor inductance
L_m	:Mutual inductance

Replacing the system of equations (2) in (1), we obtain the mathematical DSIM model (3).

$$\begin{cases} v_{s\alpha1} = R_{s1} i_{s\alpha1} + (L_{s1} + L_m)\sigma \dfrac{di_{s\alpha1}}{dt} + \\ \qquad + \dfrac{L_m L_r}{L_m + L_r} \dfrac{di_{s\alpha2}}{dt} + \dfrac{L_m}{L_m + L_r} \dfrac{d\Phi_{r\alpha}}{dt} \\ v_{s\beta1} = R_{s1} i_{s\beta1} + (L_{s1} + L_m)\sigma \dfrac{di_{s\beta1}}{dt} + \\ \qquad + \dfrac{L_m L_r}{L_m + L_r} \dfrac{di_{s\beta2}}{dt} + \dfrac{L_m}{L_m + L_r} \dfrac{d\Phi_{r\beta}}{dt} \\ v_{s\alpha2} = R_{s2} i_{s\alpha2} + (L_{s2} + L_m)\sigma \dfrac{di_{s\alpha2}}{dt} + \\ \qquad + \dfrac{L_m L_r}{L_m + L_r} \dfrac{di_{s\alpha1}}{dt} + \dfrac{L_m}{L_m + L_r} \dfrac{d\Phi_{r\alpha}}{dt} \\ v_{s\beta2} = R_{s2} i_{s\beta2} + (L_{s2} + L_m)\sigma \dfrac{di_{s\beta2}}{dt} + \\ \qquad + \dfrac{L_m L_r}{L_m + L_r} \dfrac{di_{s\beta1}}{dt} + \dfrac{L_m}{L_m + L_r} \dfrac{d\Phi_{r\beta}}{dt} \\ 0 = -\dfrac{L_m}{T_r}(i_{s\alpha1} + i_{s\alpha2}) + \dfrac{1}{T_r}\Phi_{r\alpha} + \dfrac{d\Phi_{r\alpha}}{dt} + \omega_r \Phi_{r\beta} \\ 0 = -\dfrac{L_m}{T_r}(i_{s\beta1} + i_{s\beta2}) + \dfrac{1}{T_r}\Phi_{r\beta} + \dfrac{d\Phi_{r\beta}}{dt} + \omega_r \Phi_{r\alpha} \end{cases} \quad (3)$$

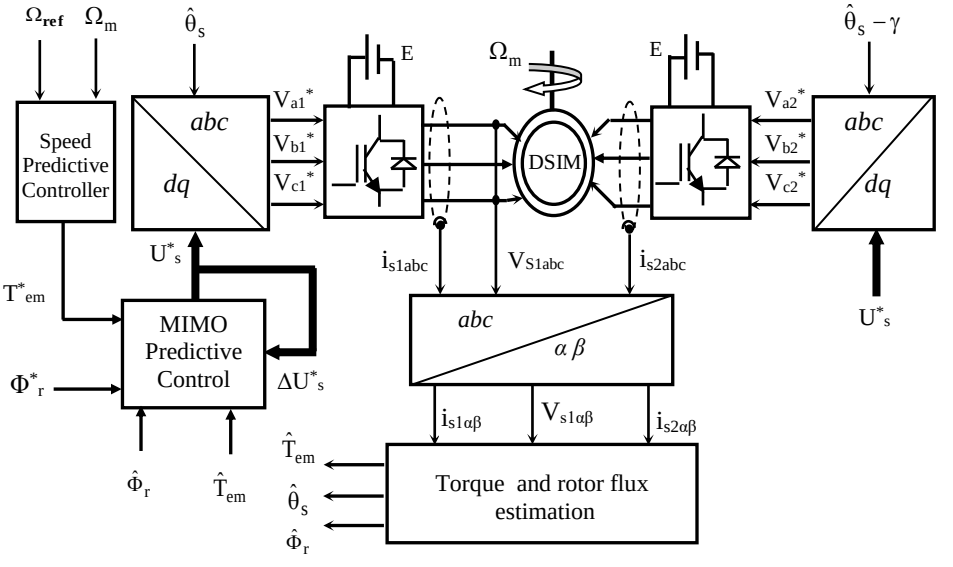

Fig. 1. MIMO Predictive control of DSIM.

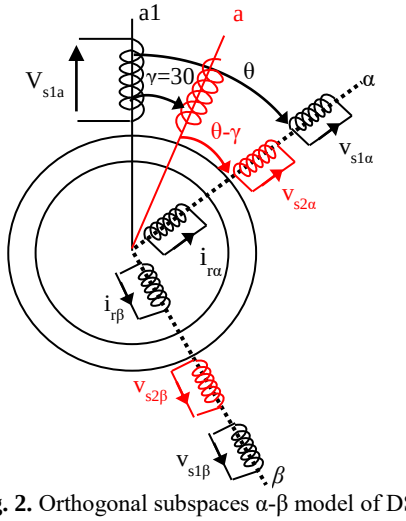

Fig. 2. Orthogonal subspaces α-β model of DSIM

With:

$$\sigma = 1 - \frac{L_m^2}{(L_m + L_r)(L_m + L_s)},$$

$$L_{s1} = L_{s2} = L_s,$$

$$T_r = \frac{L_m + L_r}{R_r}$$

Where:

σ :Total leakage factor;
T_r :Rotor time constant.

1.3. Mechanical Equations

The equation of the electromagnetic torque is [4], [12]:

$$T_{em} = p\frac{L_m}{L_m + L_r}\begin{bmatrix}(i_{s\beta 1} + i_{s\beta 2})\Phi_{r\alpha} - \\ -(i_{s\alpha 1} + i_{s\alpha 2})\Phi_{r\beta}\end{bmatrix} \quad (4)$$

Where:

T_{em} :Electromagnetique torque;
p :Number of pole pairs

The mechanical equation is:

$$J\frac{d\Omega_r}{dt} = T_{em} - T_L - k_f\Omega_r \quad (5)$$

Where:

J :Inertia;
Ω_r :Mechanical rotor speed
T_L :Load torque
k_f :Viscous friction coefficient

3. DIRECT FIELD ORIENTED CONTROL OF DSIM

Fig. 3 presents the main blocs of the direct field-oriented control of a double stator induction machine [8].

3.1. Rotor Flux Amplitude and Position Estimation of DSIM

In the direct vector control, knowledge of the rotor flux (amplitude and phase) is required to ensure the decoupling between the torque and flux. Indeed, the position of the rotor flux θ_s is calculated algebraically from the information on the rotor flux [13], [14].

$$\begin{cases}\hat{\Phi}_r = \sqrt{\Phi_{r\alpha}^2 + \Phi_{r\beta}^2} \\ \hat{\theta}_s = \text{arctg}\left(\dfrac{\Phi_{r\beta}}{\Phi_{r\alpha}}\right)\end{cases} \quad (6)$$

These components can be expressed from the DSIM voltage model; equation (3):

$$\begin{cases} \Phi_{r\alpha} = \dfrac{L_r + L_m}{L_m}\displaystyle\int \left[V_{s\alpha 1} - R_s i_{s\alpha 1} - \sigma(L_s + L_m)\frac{di_{s\alpha 1}}{dt} - \frac{L_m L_r}{L_m + L_r}\frac{di_{s\alpha 2}}{dt} \right] dt \\ \Phi_{r\beta} = \dfrac{L_r + L_m}{L_m}\displaystyle\int \left[V_{s\beta 1} - R_s i_{s\beta 1} - \sigma(L_s + L_m)\frac{di_{s\beta 1}}{dt} - \frac{L_m L_r}{L_m + L_r}\frac{di_{s\beta 2}}{dt} \right] dt \end{cases} \quad (7)$$

3.2. The Rotor Flux Orientation

The principle of the orientation shown in Fig. 4 aligns the rotor flux on the direct axis of Park's axes [4], [12].

Thus, we obtain the orientation of the rotor flux:

$$\begin{cases} \Phi_r = \Phi_{rd} \\ \Phi_{rq} = 0 \end{cases} \quad (8)$$

The following equations of rotor flux and electromagnetic torque are used:

$$\begin{cases} \dfrac{d\Phi^*_r}{dt} = \dfrac{1}{T_r}\left[L_m (i^*_{sd1} + i^*_{sd2}) - \Phi^*_r \right] \\ T^*_{em} = p\dfrac{L_m}{L_m + L_r}\left[(i^*_{sq1} + i^*_{sq2})\Phi^*_r \right] \end{cases} \quad (9)$$

After the Laplace transform, we can write:

$$\begin{cases} \Phi^*_r = \dfrac{L_m}{1 + T_r s}(i^*_{sd1} + i^*_{sd2}) \\ T^*_{em} = p\dfrac{L_m}{L_m + L_r}\left[(i^*_{sq1} + i^*_{sq2})\Phi^*_r \right] \end{cases} \quad (10)$$

The two stator windings are identical, so the powers provided by this two windings system are the same, hence:

$$\begin{cases} i^*_{sd1} = i^*_{sd2} = \dfrac{1 + T_r s}{2L_m}\Phi^*_r \\ i^*_{sq1} = i^*_{sq2} = p\dfrac{L_m + L_r}{2L_m \Phi^*_r} T^*_{em} \end{cases} \quad (11)$$

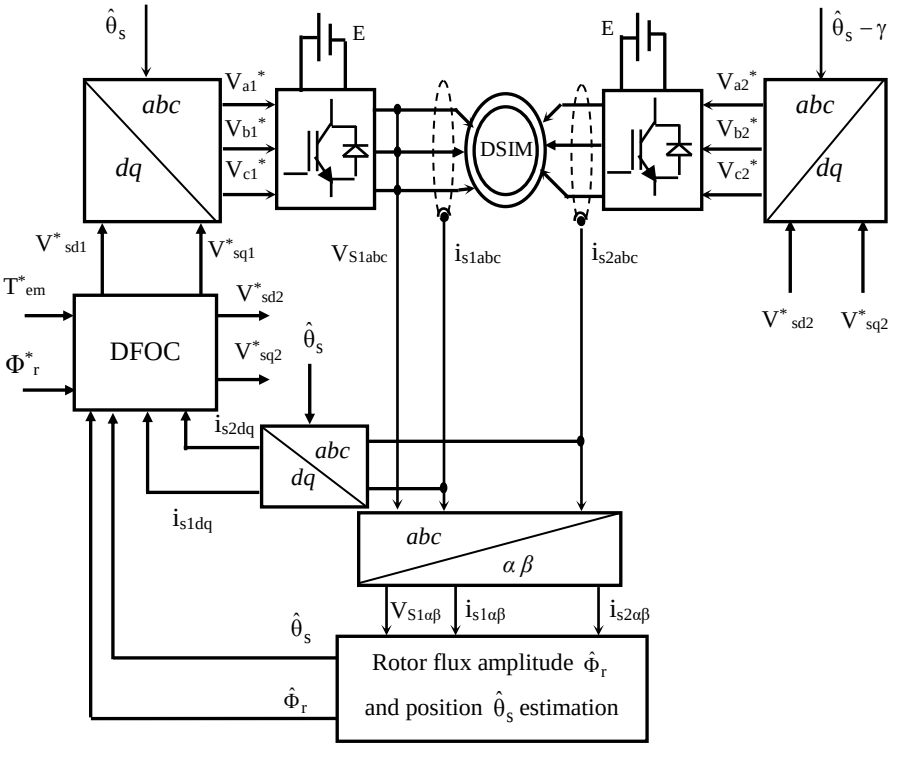

Fig. 3. The direct field-oriented control scheme of DSIM.

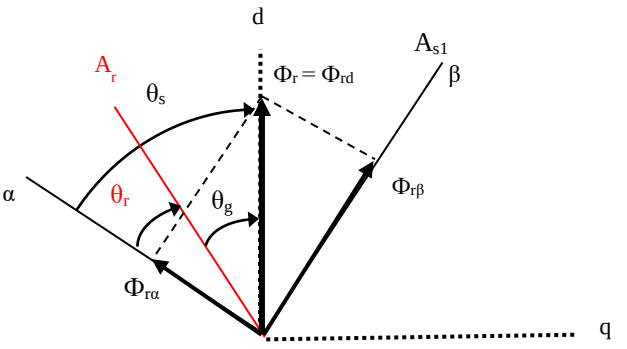

Fig. 4. Space vector diagram for rotor flux orientation.

3.3. The Compensation Method

The compensation method is concerned with the regulation of four currents loops while neglecting the coupling terms [13].

Four new independent voltages V^{r}_{ds1}, V^{r}_{qs1}, V^{r}_{ds2}, V^{r}_{qs2} are introduced to the decoupling such that:

$$\begin{cases} V^{*}_{sd1} = V^{c}_{ds1} + V^{r}_{ds1} \\ V^{*}_{sq1} = V^{c}_{qs1} + V^{r}_{qs1} \\ V^{*}_{sd2} = V^{c}_{ds2} + V^{r}_{ds2} \\ V^{*}_{sq2} = V^{c}_{qs2} + V^{r}_{qs2} \end{cases} \quad (12)$$

The compensation voltages at the regulator's output are given by [4]:

$$\begin{cases} V^{c}_{ds1} = -\hat{\omega}_s \left[L_{s1} i_{sq1} + \dfrac{L_r}{R_r} \omega_g \Phi_r \right] \\ V^{c}_{qs1} = \hat{\omega}_s \left[L_{s1} i_{sd1} + \Phi_r \right] \\ V^{c}_{ds2} = -\hat{\omega}_s \left[L_{s2} i_{sq2} + \dfrac{L_r}{R_r} \omega_g \Phi_r \right] \\ V^{c}_{qs2} = \hat{\omega}_s \left[L_{s2} i_{sd2} + \Phi_r \right] \end{cases} \quad (13)$$

The references control voltages V^{*}_{sd1}, V^{*}_{sq1}, V^{*}_{sd2} and V^{*}_{sq2} are reconstructed from voltages V^{c}_{ds1}, V^{c}_{qs1}, V^{c}_{ds2} and V^{c}_{qs2}.

We define a new system to which the actions of the *d* and *q* axes are decoupled:

$$\begin{cases} V^{r}_{ds1} = R_{s1} i_{sd1} + L_{s1} \dfrac{di_{sd1}}{dt} \\ V^{r}_{qs1} = R_{s1} i_{sq1} + L_{s1} \dfrac{di_{sq1}}{dt} \\ V^{r}_{ds2} = R_{s2} i_{sd2} + L_{s2} \dfrac{di_{sd2}}{dt} \\ V^{r}_{qs2} = R_{s2} i_{sq2} + L_{s2} \dfrac{di_{sq2}}{dt} \end{cases} \quad (14)$$

After the Laplace transform, we can write:

$$\begin{cases} V^{r}_{ds1} = (R_{s1} + sL_{s1}) i_{sd1} \\ V^{r}_{qs1} = (R_{s1} + sL_{s1}) i_{sq1} \\ V^{r}_{ds2} = (R_{s2} + sL_{s2}) i_{sd2} \\ V^{r}_{qs2} = (R_{s2} + sL_{s2}) i_{sq2} \end{cases} \quad (15)$$

For a perfect decoupling, adding the current control loops i_{sd1}, i_{sq1}, i_{sd2} and i_{sq2}, we obtain at their output the voltages V^{r}_{ds1}, V^{r}_{qs1}, V^{r}_{ds2} and V^{r}_{qs2}.

4. MULTIVARIABLE PREDICTION CONTROL

The monovariable predictive control is a simple extension of multivariable predictive control [13]. In contrast to the monovariable system, the resulting output / input transfer for a multivariable system is a transfer matrix [14].

4.1. Multivariable Systems

The multivariable system, as shown in Fig. 5, states the model given by [15];

$$\begin{cases} \dot{x}(k) = A.x(k) + B.u(k) & x(k_0) = x_0 \\ y(k) = C.x(k) + D.u(k) \end{cases} \quad (24)$$

Where $x \in R^{n}, u \in R^{m}$ et $y \in R^{r}$

Due to the linearity of the z operator, it is possible to apply it to equations (24)

$$\begin{cases} z.X(z) - x_0 = A.X(z) + B.U(z) \\ Y(z) = C.X(z) + D.U(z) \end{cases} \quad (25)$$

Where $X(z) = Z[x(k)], U(z) = Z[u(k)]$ et $Y(z) = Z[y(k)]$.

By solving the equations (25) it comes:

$$Y(z) = \left[C(z.I - A)^{-1} B + D \right] U(z) = G(z) U(z) \quad (26)$$

Where:

$$G(z^{-1}) = \left[C(z.I - A)^{-1} B + D \right]$$

The matrix $G(z) \in C^{nXm}$ is called the transfer matrix linking the input $U(z)$ to the output $Y(z)$ [16].

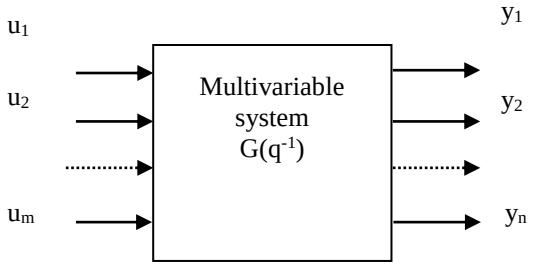

Fig. 5. The multivariable system of *m* inputs and *n* outputs.

4.2. System Matrix Determination

However, if the system is a multidimensional, then $A(q^{-1})$ and $B(q^{-1})$ are transfer matrices. Since $G(q^{-1})$ is also a transfer matrix, the polynomials $A(q^{-1})$ and $B(q^{-1})$ cannot be simply determined by taking the denominator and the numerator of $G(q^{-1})$.

A simple method for the determination of $A(q^{-1})$ and $B(q^{-1})$ is presented by Camacho in [10], thus a very good detailed description could also be found in the Geering publication [17].

For simplicity reasons, only the method of Camacho [10] is treated.

We have:

$$G(q^{-1}) = A(q^{-1})^{-1}.B(q^{-1}).q^{-1} \quad (27)$$

Now the simplest is to assume that $A(q^{-1})$ is a diagonal matrix whose diagonal elements are the smallest common multiples of the denominators of the corresponding lines of $G(q^{-1})$, and the transfer matrix $B(q^{-1})$ can simply be computed with:

$$B(q^{-1}) = A(q^{-1}).G(q^{-1}).q \quad (28)$$

4.3. The Multivariable CARIMA Model

Analog to the monovariable system, the following approach is taken for the CARIMA model [18]:

$$A(q^{-1})y(k) = q^{-d}\, B(q^{-1})\, u(k) + \frac{C(q^{-1})}{\Delta}\zeta(k) \quad (29)$$

Where:

$$\begin{cases} A(q^{-1}) = I + A_1 q^{-1} + A_2 q^{-2} + ... + A_{na} q^{-na} \\ B(q^{-1}) = B_0 + B_1 q^{-1} + B_2 q^{-2} + ... + B_{nb} q^{-nb} \\ C(q^{-1}) = I + C_1 q^{-1} + C_2 q^{-2} + ... + C_{nc} q^{-nc} \end{cases} \quad (30)$$

The dimensions of the individual matrices are:

$A(q^{-1})$: (n X n) Matrix;
$B(q^{-1})$: (n X m) Matrix;
$C(q^{-1})$: (n X n) Matrix;
$y(k)$: (n X 1) Vector;
$u(k)$: (m X 1) Vector;
$\zeta(k)$: (n X 1) Vector.

With:

n : The number of system outputs.
m : The number of system inputs.

4.4. The J-Step Ahead Multivariable Predictor

As in SISO case, a matrix Diophantine equation is used for calculating the matrix predictor [19,20]:

$$A_m(q^{-1}).C(q^{-1}) = \Delta(q^{-1})A(q^{-1})F_j(q^{-1}) + q^{-d-j}G_j(q^{-1}) \quad (31)$$

With:

$$F_j(q^{-1}) = F_{j,0} + F_{j,1}q^{-1} + F_{j,2}q^{-2} + ... + F_{j,j-1}q^{-(j-1)}$$
$$G_j(q^{-1}) = G_{j,0} + G_{j,1}q^{-1} + G_{j,2}q^{-2} + ... + G_{j,na}q^{-na}$$
$$A_m(q^{-1}) = A_0 + A_1 q^{-1} + A_2 q^{-2} + ... + A_{nAm} q^{-nAm}$$

Where:
$F_j(q^{-1})$: (n X n) Matrix;
$G_j(q^{-1})$: (n X n) Matrix ;
$A_m(q^{-1})$: (n X n) Matrix ;

After resolving equation (31) for $\Delta A(q^{-1})F_j(q^{-1})$ and after inserting the result in equation (30) which has been multiplied by $\Delta F_j(q^{-1})q^j$, the prediction equation can be obtained:

$$\begin{aligned} A_m(q^{-1})C(q^{-1})\hat{y}(k+j) &= G_j(q^{-1})y(k) + \\ &+ B(q^{-1})F_j(q^{-1})\Delta u(k+j-d) + C(q^{-1})F_j(q^{-1})\ \zeta(k+j) \end{aligned} \quad (32)$$

All noise terms are in the future, too, which means they are not known and they can be neglected. Therefore, the best prediction is [9], [14]:

$$\begin{aligned} A_m(q^{-1})C(q^{-1})\hat{y}(k+j) &= G_j(q^{-1})y(k) + \\ &+ B(q^{-1})F_j(q^{-1})\Delta u(k+j-d) \end{aligned} \quad (33)$$

And as:

$$B(q^{-1})F_j(q^{-1}) = H_j(q^{-1}).A_m(q^{-1}).C(q^{-1}) + q^{-j-1}J_j(q^{-1}) \quad (34)$$

Where, in contrary the one-dimensional case, $H_j(q^{-1})$ is a transfer matrix, the part forming the free response is completely inside the term $q^{-j-1}J_j(q^{-1})$.

$$A_m(q^{-1})C(q^{-1})\hat{y}(k+j) = \underbrace{A_m(q^{-1})C(q^{-1})H_j(q^{-1})\ \Delta u(k+j-d)}_{\text{forced response}} + \overbrace{G_j(q^{-1})y(k)+J_j(q^{-1})\ \Delta u(k-1)}^{\text{free response}} \quad (35)$$

Thus, the prediction equation becomes:

$$\hat{y}(k+j) = \underbrace{H_j(q^{-1})\ \Delta u(k+j-d)}_{\text{forced response}} + \overbrace{E(k+j)}^{\text{free response}} \quad (36)$$

Where:

$$E(k+j) = \frac{G_j(q^{-1})y(k)+J_j(q^{-1})\ \Delta u(k-1)}{A_m(q^{-1})C(q^{-1})}$$

With:

$H_j(q^{-1})$, $J_j(q^{-1})$: (n X m) Matrix;

$E(k)$: (n X 1) Vector.

Therefore, the j-step predictions for a MIMO system are:

$$\begin{cases} \hat{y}(k+1) = H_1(q^{-1})\ \Delta u(k+1-d)+E(k+1) \\ \hat{y}(k+2) = H_2(q^{-1})\ \Delta u(k+2-d)+E(k+2) \\ \hat{y}(k+3) = H_3(q^{-1})\ \Delta u(k+3-d)+E(k+3) \\ \vdots \\ \hat{y}(k+N_2) = H_{N_2}(q^{-1})\ \Delta u(k+N_2-d)+E(k+N_2) \end{cases}$$

Similar to the monovariable system, the term $H_j(q^{-1})\ \Delta u(k+j-d)$ of equation (36) is associated with a multiplication of real matrices $H.U$. So:

$$Y = H.U + E \quad (37)$$

A quadratic cost function is applied to the prediction values of (37) to compute an optimal sequence of the control signal [9].

The cost function is the same as for the one-dimensional control [20].

$$J_{GPC} = \sum_{j=N_1}^{N_2} \left\| \hat{y}(k+j) - \omega_{ref}(k+j) \right\|^2 + \lambda \sum_{j=1}^{N_u} \left\| \Delta u(k+j-d) \right\|^2 \quad (38)$$

As in the one-dimensional case, a multi-dimensional cost function can be implemented by substituting (37) into (38):

$$J_{GPC} = (HU+E-W)^T(HU+E-W)+\lambda U^T U \quad (39)$$

In order to minimize this equation, it is first developed in distinct terms [19-20]:

$$J_{GPC} = U^T(H^TH+\lambda I)U + U^TH^T(E-W) + (E-W)^THU + (E-W)^T(E-W) \quad (40)$$

Due to the identity:

$$U^TH^T(E-W) = (E-W)^THU \quad (41)$$

J_{GPC} can be further simplified by:

$$J_{GPC} = U^T(H^TH+\lambda I)U + 2U^TH^T(E-W) + (E-W)^T(E-W) \quad (42)$$

The analytic minimization $\frac{dJ_{GPC}}{dU} \overset{!}{=} 0$ gives [21], [22]:

$$\tilde{U} = \left(H^TH+\lambda I_{N_u}\right)^{-1}H^T(W-E) \quad (43)$$

5. MULTIVARIABLE PREDICTION CONTROL OF DSIM

The objective of this control strategy is to control simultaneously the electromagnetic torque and the rotor flux norm. The multivariable predictive control law developed in section (5) is used to track trajectories (torque and flux norm) to generate the reference voltages (Fig. 6).

5.1. Synthesis of the MIMO Predictive Control law

The multivariable predictive control for the DSIM drive can be designed (Fig. 7).

In our case the selected outputs and inputs are:

$$Y = \begin{bmatrix} \Phi_r \\ T_{em} \end{bmatrix}, \qquad \hat{Y} = \begin{bmatrix} \hat{\Phi}_r \\ \hat{T}_{em} \end{bmatrix} \text{ and } U_s^r = \begin{bmatrix} V_{ds}^r \\ V_{qs}^r \end{bmatrix}$$

The prediction of the outputs is given by equation (44):

$$\begin{bmatrix} \hat{\Phi}_r(k+j) \\ \hat{T}_{em}(k+j) \end{bmatrix} = G_j(q^{-1}) \begin{bmatrix} \Phi_r(k) \\ T_{em}(k) \end{bmatrix} + H_j(q^{-1}) \begin{bmatrix} \Delta V_{sd}(k+j-1) \\ \Delta V_{sq}(k+j-1) \end{bmatrix} + J_j(q^{-1}) \begin{bmatrix} \Delta V_{sd}(k-1) \\ \Delta V_{sq}(k-1) \end{bmatrix} \quad (44)$$

With:

$H_j(q^{-1})$, $J_j(q^{-1})$: (2 X 2) Matrix;

$G_j(q^{-1})$: (2 X 2) Matrix.

The prediction model is assumed to be linear time invariant model (LTI), modeling the dynamic interactions between two sets of inputs (V_{sd}, V_{sq}) and two sets of outputs (Φ_r, T_{em}).

Since from reference flux Φ_r^* and reference torque T^*_{em}, the reference currents (I^*_{ds} et I^*_{qs}) can be deduced directly from the equations of the system (45).

$$\begin{cases} \Phi_r^* = \dfrac{2L_m}{1+T_r s} I_{ds}^* \\ T_{em}^* = \dfrac{2pL_m}{L_m + L_r} \Phi_r^* I_{qs}^* \end{cases} \quad (45) \qquad \begin{cases} I_{ds}^* = \dfrac{1}{R_{s1} + sL_{s1}} V_{ds}^r \\ I_{qs}^* = \dfrac{1}{R_{s1} + sL_{s1}} V_{qs}^r \end{cases} \quad (46)$$

The reference voltages V_{ds}^r and V_{qs}^r are then reconstituted from the currents I^*_{ds} and I^*_{qs} by:

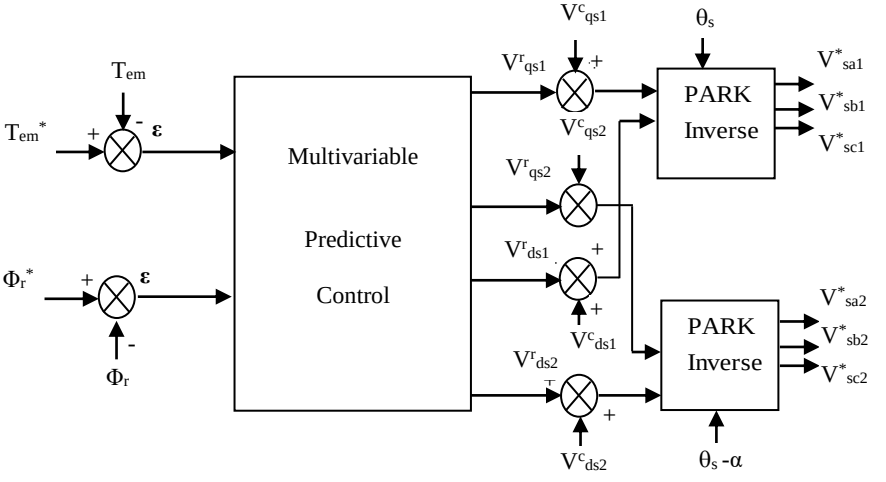

Fig. 6. Block diagram of the multivariable predictive control.

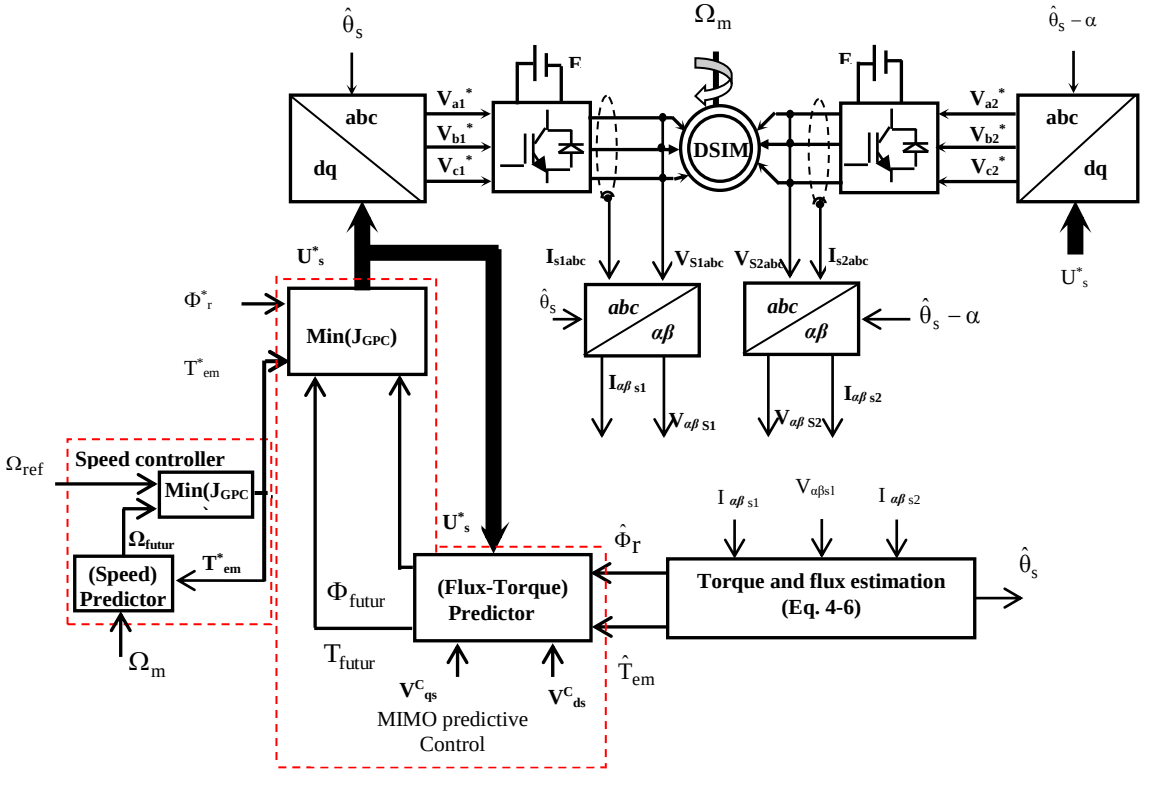

Fig. 7. Block diagram of the MIMO predictive control of DSIM.

Taking into account that the rotor flux is kept constant at its reference value, the substitution of (46) into (45) gives:

$$\begin{cases} \Phi_r^* = \dfrac{2L_m}{(1+T_r s)(R_{s1}+sL_{s1})} V_{ds}^r \\ T_{em}^* = \dfrac{2pL_m}{(L_m+L_r)(R_{s1}+sL_{s1})} V_{qs}^r \end{cases} \quad (47)$$

According to the system (12), the reference voltages are decomposed by two voltage vectors:

$$\begin{cases} V_{ds}^r = V_{ds}^* - V_{ds}^c \\ V_{qs}^r = V_{qs}^* - V_{qs}^c \end{cases} \quad ; \quad U_s^* = \begin{bmatrix} V_{ds}^* & V_{qs}^* \end{bmatrix} \quad (48)$$

The rewriting of (47) in the matrix form gives:

$$\begin{bmatrix} \Phi_r^* \\ T_{em}^* \end{bmatrix} = \begin{bmatrix} G_{11}(s) & 0 \\ 0 & G_{22}(s) \end{bmatrix} \begin{bmatrix} V_{ds}^r \\ V_{qs}^r \end{bmatrix} \quad (49)$$

With:

$$\begin{cases} G_{11}(s) = \dfrac{2L_m}{(1+T_r s)(R_{s1}+sL_{s1})} \\ G_{22}(s) = \dfrac{2pL_m}{(L_m+L_r)(R_{s1}+sL_{s1})} \end{cases} \quad (50)$$

For a sampling period T_e = 0.001sec, the discrete transfer matrix is:

$$G_p(q^{-1}) = \begin{bmatrix} G_{11}(q^{-1}) & 0 \\ 0 & G_{22}(q^{-1}) \end{bmatrix} = q^{-1} \begin{bmatrix} \dfrac{(8.95+8.44q^{-1}).10^{-5}}{1-0.84q^{-1}+0.84q^{-2}} & 0 \\ 0 & \dfrac{0.082}{1-0.84q^{-1}} \end{bmatrix} \quad (51)$$

The polynomials matrices of the CARIMA model (29) are:

$$\begin{cases} A(q^{-1}) = \begin{bmatrix} (1-0.84q^{-1}+0.84q^{-2}).(1-0.84q^{-1}) & 0 \\ 0 & (1-0.84q^{-1}+0.84q^{-2}).(1-0.84q^{-1}) \end{bmatrix} \\ B(q^{-1}) = \begin{bmatrix} (8.95+8.44q^{-1})(1-0.84q^{-1}).10^{-5} & 0 \\ 0 & 0.082(1-0.84q^{-1}+0.84q^{-2}) \end{bmatrix} \\ C(s) = \begin{bmatrix} 1 & 0 \\ 0 & 1 \end{bmatrix} \end{cases} \quad (52)$$

The matrix form of the prediction equation (44) for j = 1 is:

$$\begin{cases} \begin{bmatrix} \hat{\Phi}_r(k+1) \\ \hat{T}_{em}(k+1) \end{bmatrix} = \begin{bmatrix} 1.84-1.68q^{-1}+0.84q^{-2} & 0 \\ 0 & 1.84-1.68q^{-1}+0.84q^{-2} \end{bmatrix} \begin{bmatrix} \Phi_r(k) \\ T_{em}(k) \end{bmatrix} + \\ + \begin{bmatrix} 8.95.10^{-5}-7.0896.10^{-5}q^{-2} & 0 \\ 0 & 8.95.10^{-5}-7.0896.10^{-5}q^{-2} \end{bmatrix} \begin{bmatrix} \Delta V_{ds}^r(k) \\ \Delta V_{qs}^r(k) \end{bmatrix} + \\ + \begin{bmatrix} 8.4399 & 0 \\ 0 & 8.4399 \end{bmatrix} \begin{bmatrix} \Delta V_{ds}^r(k-1) \\ \Delta V_{qs}^r(k-1) \end{bmatrix} \end{cases} \quad (53)$$

Where:

$$\begin{cases} G_1(q^{-1}) = \begin{bmatrix} 1.84 - 1.68q^{-1} + 0.84q^{-2} & 0 \\ 0 & 1.84 - 1.68q^{-1} + 0.84q^{-2} \end{bmatrix} \\ H_1(q^{-1}) = \begin{bmatrix} 8.95.10^{-5} - 7.0896.10^{-5}q^{-2} & 0 \\ 0 & 8.95.10^{-5} - 7.0896.10^{-5}q^{-2} \end{bmatrix} \\ J_1(q^{-1}) = \begin{bmatrix} 8.4399 & 0 \\ 0 & 8.4399 \end{bmatrix} \end{cases} \quad (54)$$

The multivariable cost function is defined by equation (42):

$$J_{GPC} = U^T(H^TH + \lambda I)U + 2U^TH^T(E - W) + \\ + (E - W)^T(E - W) \quad (55)$$

The analytic minimization $\frac{dJ_{GPC}}{d\tilde{U}} \overset{!}{=} 0$ gives:

$$\tilde{U} = \left(H^TH + \lambda I_{N_u}\right)^{-1}H^T\left(W - E\right) \quad (56)$$

With:

$$W = \begin{bmatrix} \begin{bmatrix} \Phi_r^*(k+1) \\ T_{em}^*(k+1) \end{bmatrix} \\ \vdots \\ \vdots \\ \begin{bmatrix} \Phi_r^*(k+j) \\ T_{em}^*(k+j) \end{bmatrix} \end{bmatrix}, \quad U = U_s^* = \begin{bmatrix} \begin{bmatrix} \Delta V_{ds}^r(k) \\ \Delta V_{qs}^r(k) \end{bmatrix} \\ \vdots \\ \vdots \\ \begin{bmatrix} \Delta V_{ds}^r(k+j-1) \\ \Delta V_{qs}^r(k+j-1) \end{bmatrix} \end{bmatrix}$$

$$E = G(q^{-1})\begin{bmatrix} \Phi_r(k) \\ T_{em}(k) \end{bmatrix} + J(q^{-1})\begin{bmatrix} \Delta V_{ds}^r(k-1) \\ \Delta V_{qs}^r(k-1) \end{bmatrix}$$

and:

$$G(q^{-1}) = \begin{bmatrix} G_1(q^{-1}) \\ \vdots \\ \vdots \\ G_j(q^{-1}) \end{bmatrix}; \quad J(q^{-1}) = \begin{bmatrix} J_1(q^{-1}) \\ \vdots \\ \vdots \\ J_j(q^{-1}) \end{bmatrix};$$

$$H(q^{-1}) = \begin{bmatrix} H_1(q^{-1}) & 0 & 0 & 0 \\ H_2(q^{-1}) & H_1(q^{-1}) & 0 & 0 \\ \vdots & \cdots & H_1(q^{-1}) & 0 \\ H_j(q^{-1}) & \cdots & H_2(q^{-1}) & H_1(q^{-1}) \end{bmatrix}$$

5.2. Synthesis of the SISO Predictive Control law

The prediction model is given by the following mechanical equation [13], [20]:

$$\frac{\Omega_m}{T_{em}^*} = \frac{k_m}{1 + T_m s} \quad (57)$$

With:

$$k_m = \frac{1}{k_f} \; ; \; T_m = \frac{J}{k_f}$$

For $k_m = 1000$; $T_m = 62.5$ and $T_e = 0.001$sec, equation (57) is represented by the following discrete transfer function:

$$\frac{\Omega_m(k)}{T_{em}^*(k)} = \frac{0.016q^{-1}}{1 - q^{-1}} \quad (58)$$

The speed prediction equation is given by:

$$\Omega_m^*(k+j) = G_j(q^{-1})\Omega_m(k) + J_j(q^{-1})\Delta T_{em}(k-1) + \\ + H_j(q^{-1})\Delta T_{em}(k+j) \quad (59)$$

The future T_{em} command is:

$$\tilde{T}_{em} = [H^TH + \lambda I_{N_u}]^{-1}H^T[\Omega_{ref} - G(q^{-1})\Omega_m(k) - \\ - J(q^{-1})\Delta T_{em}(k-1)] \quad (60)$$

With:

$$H = \begin{bmatrix} 0 & 0 & 0 \\ 0.0160 & 0 & 0 \\ 0.0320 & 0.0160 & 0 \end{bmatrix}; G = \begin{bmatrix} 2 & -1q^{-1} \\ 3 & -2q^{-1} \\ 4 & -3q^{-1} \end{bmatrix} \text{ and}$$

$$J = \begin{bmatrix} 0.016 \\ 0.032 \\ 0.048 \end{bmatrix}$$

6. SIMULATION RESULTS

Using the block diagram of Fig. 7, the simulation was carried out under the same conditions as the conventional FOC control with the following adjustment parameters:

Table 1. Predictive control setting parameters.

Predictive regulators / Parameter	MIMO_Predictive (Torque/Flux Norm)	SISO_Predictive (Speed)
N1	1	1
N2	5	5
Nu	3	3
λ	Matrix 0.01 $\mathbf{I_{X2}}$	0.002

6.1. Discussion

At start-up and during the transient regime (Fig. 8), the speed increases linearly as a function of time and reaches its reference value *288rd / sec* at *t = 0.75sec* without overshoot. The electromagnetic torque of the DSIM reaches its maximum value at start-up and then reaches the steady state at *t = 0.75sec*. At the beginning, the stator current I_{s1a} reaches a current of *33A*. The stator voltage V_{s1a} is sinusoidal in shape. The rotor flux norm presents at the start-up some peaks for a fraction of a second oscillating around their setpoints. At time *t = 2.5sec*, the speed reverses and reaches its negative setpoint after *1.2sec* without any overshoot. This generates an increase in the current I_{s1a} of a magnitude equal to that recorded during the start-up, which stabilizes after 1.2sec, the electromagnetic torque reaches its maximum value at the time of the inversion of the speed, which stabilizes once the latter reaches its setpoint (*-288rd / sec*); the torque T_{futur} progresses in a manner analogous to the reference torque; the flux norm Φ_{future} follows their reference value during the inversion of the speed.

6.2. Robustness Test

Figs. (9.1) to (9.4) respectively show the no load characteristics of the DSIM with speed and flux norm regulation by a multivariable predictive control, followed by increasing the rotor resistance, stator resistance and decreasing the mutual inductance *75%* of its nominal values, and an increase in the inertia *200%* of its nominal value between *t = 1.5sec* and *t = 2sec*.

The simulations results show clearly the insensitivity of the predictive control to the variation of the mutual inductance. On the contrary, we note that a 75% increase in the value of the rotor resistance, stator resistance and inertia, has a little influence on the performance. We notice (Fig. 10) a slight decrease in speed and a slight increase in the flux norm for a simultaneous variation of + 75% Rr, + 75% Rs, -75% Lm and + 200% J .

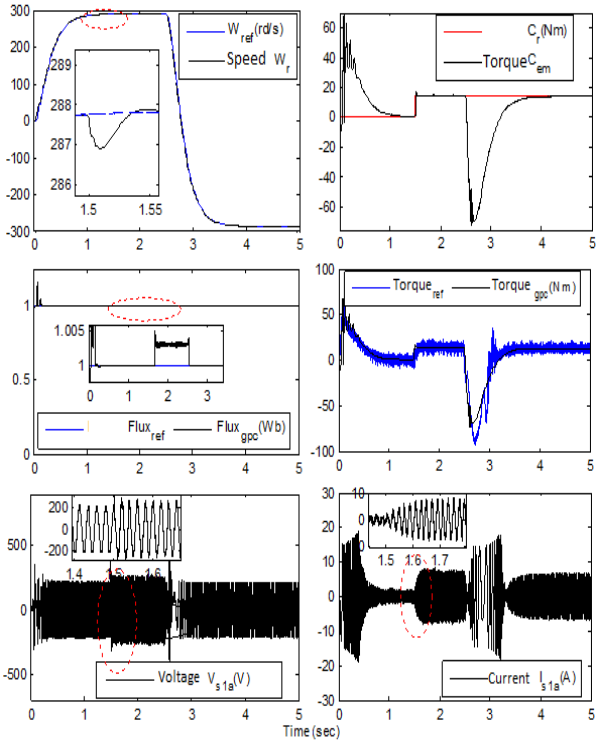

Fig.8. Simulation results for MIMO predictive control of DSIM.

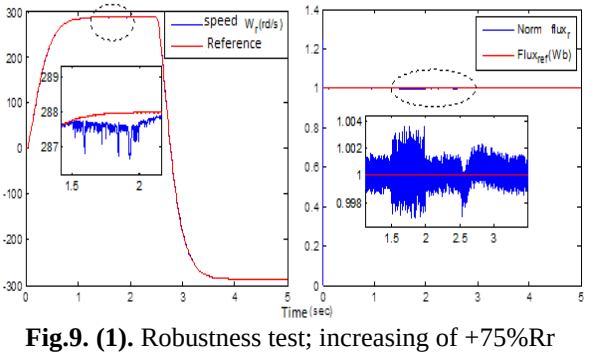

Fig.9. (1). Robustness test; increasing of +75%Rr (speed and rotor flux norm results).

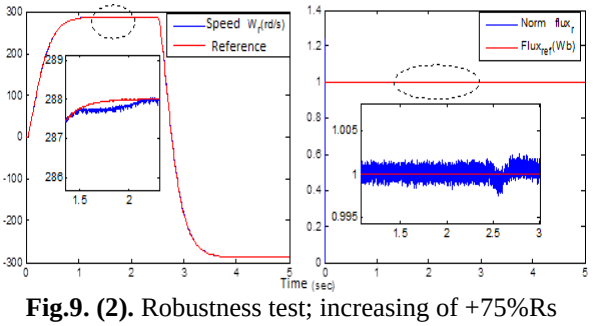

Fig.9. (2). Robustness test; increasing of +75%Rs (speed and rotor flux norm results).

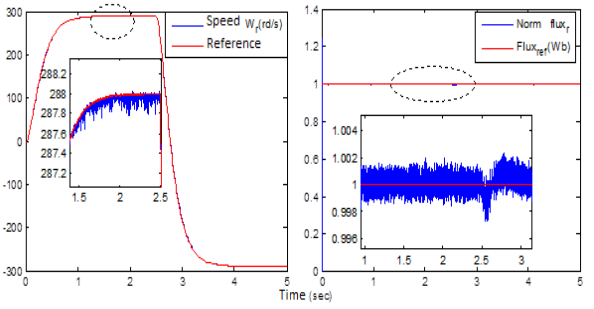

Fig. 9. (3). Robustness test; decreasing of -75% L_m (speed and rotor flux norm results).

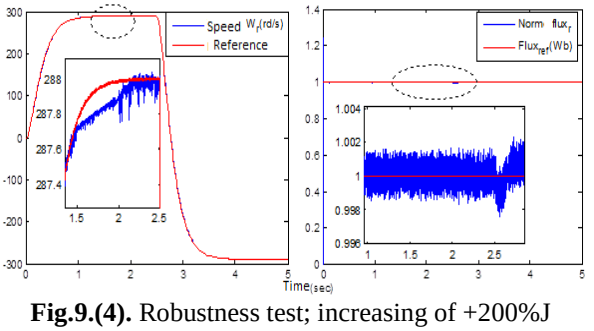

Fig.9.(4). Robustness test; increasing of +200%J (speed and rotor flux norm results).

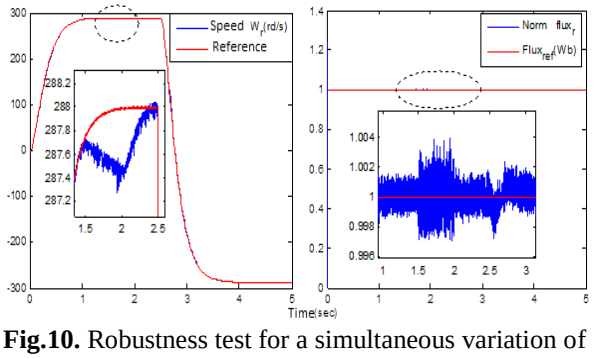

Fig.10. Robustness test for a simultaneous variation of +75%(Rs,Rr), -75%Lm and +200%J (speed and rotor flux norm results).

7. CONCLUSION

In this paper we presented the predictive control, based speed, torque and flux prediction of Double Stator Induction Machine (DSIM). Then we discussed the basic idea of multivariable predictive control as a decoupling system able to replace the conventional FOC control and allowing to control the future torque and the future flux to minimize the reference voltages, such as the synthesis of this control takes into account all the components of the drive system. (Machine, Inverters and System estimation). From this fact, it is concluded that the adjustment of the speed, the flux and the torque by the predictive control, brings remarkable improvements over the conventional control. In addition, the decoupling between the flux and the electromagnetic torque is perfectly ensured.

The prediction operation of the speed, the flux and the torque increases reliability, reduces the complexity and the cost of the system. Indeed, the speed variation of the double star induction machine in variable speed range is a difficult problem to be overcome with respect to the parametric variation and in particular the mutual inductance, the rotor resistance and the stator resistors, thus causing the instability of the system.

From the obtained results, it can be concluded that the studied techniques are valid for the nominal conditions, even satisfying the operations in variable speed drive and even when the machine is loaded, on the other hand they have acceptable robustness to the variation of the load, thus achieving good static and dynamic performance.

8. APPENDIX

Double stator induction motor parameters [3], [4], [12], [20]

P_n=4.5kW, f=50Hz, $V_{n(\Delta/Y)}$=220/380V, $I_{n(\Delta/Y)}$=6.5A, Ω_n=2751rpm, p=1

R_{s1}= R_{s2}=3.72Ω, R_r =2.12Ω, L_{s1}= L_{s2}= 0.022H, L_r = 0.006H, L_m =0.3672H

J =0.0625 Kgm^2, K_f =0.001 Nm(rad/s)$^{-1}$

REFERENCES

[1] B. Ghalem, A. Bendiabdellah, "**Six-Phase Matrix Converter Fed Double Star Induction Motor",** *Journal of Applied Sciences, Acta Polytechnica Hungarica*, Vol.7, (03), pp. 163-176, 2010.

[2] Alfredo R. Muñoz, Thomas A. Lipo, Fellow, **"Dual Stator Winding Induction Machine Drive"**, *IEEE Trans. Ind App*, Vol.36,(5), pp. 1369-1380, 2000.

[3] H. Khouidmi, A. Massoum and A. Meroufel**, "Dual Star Induction Motor Drive: Modelling, Supplying and Control"**, *International Journal of Electrical and Power Engineering*, Vol. 5, pp. 28-34, 2011.

[4] R. Sadouni, A. Meroufel, **"Indirect Rotor Field-oriented Control (IRFOC) of a Dual Star Induction Machine (DSIM) Using a Fuzzy Controller",** *Journal of Applied Sciences, Acta Polytechnica Hungarica*, Vol. 9, (04), pp. 177-192, 2012.

[5] Blaschke, F., **"The Principle Of Field Orientation Applied to the New Trans-Vector Closed-Loop Control System for Rotating Field Machines"**, *Siemens-Review 39*, pp. 217-220, 1972.

[6] A. Khedher, MF. Mimouni, N. Derbel, A. Masmoudi, "**Sensorless-Adaptive DTC of Double Star Induction Motor**", *Energy Convers Manage*, 51, pp. 2878–2892, 2010.

[7] E. Y. Y. HO and P. C. SEN, **"Decoupling Control of Induction Motor Drives,"** *IEEE Trans. Ind. Elect.*, Vol. 35, (2), pp. 253–262, 1988.

[8] M. Menaa, O. Touhami, R. Ibtiouen, M. Fadel, **"Sensorless Direct Vector Control of An Induction Motor**", *Control Engineering Practice*, Vol. 16, pp. 67-77, 2008.

[9] D.W. Clarke, C. Mohtadi, P.S. Tuffs, **"Generalized Predictive Control",** *parts 1 and 2, Automatica 23,* pp. 137–160, 1987.

[10] E. Camacho, E, C. Borbons, C, **"Model Predictive Control",** *Springer-Verlag, London,* 1999.

[11] J. Richalet, A. Rault, J.L. Testud and J. Papon, **"Model Predictive Heuristic Control: Applications to Industrial Processes",** *Automatica,* Vol. 14, pp. 413– 428, 1978.

[12] H. Khouidmi, A. Massoum, **"Reduced-order Sliding Mode Observer Based Speed Sensorless Vector Control of Double Stator Induction Motor",** *Journal of Applied Sciences, Acta Polytechnica Hungarica*, Vol. 11, No. 6, pp. 229-249, 2014.

[13] H. Khouidmi, A. Massoum, A. Meroufel and B. Meliani, **"Generalized Predictive Speed Controller of Double Stator Induction Motor",** *Journal of Electrical Engineering*, Vol. 12, No. 4, 2012.

[14] G. Torkel, L. Lennart, **"Control Theory: Multivariable and Nonlinear Methods",** *Taylor & Francis Press*, London, 2000.

[15] O. N. Gasparyan, **"Linear and Nonlinear Multivariable Feedback Control: A Classical Approach",** *John Wiley & Sons Press*, England, 2008.

[16] D. Valério, J. S. Costa, "**Tuning of Fractional Controllers Minimising H2 and H∞ Norms",** *Journal of Applied Sciences, Acta Polytechnica Hungarica*, Vol. 3, No. 4, pp. 55-70, 2006.

[17] H.P. Geering, **"Berechnung von Zustandsraummodellen minimaler Ordnung aus der ¨Ubertragungsmatrix G(s) (Calculation of State Space Models with Minimal Order from the Transfer Matrix G(s))"**, *IMRT Press, Zurich*, 1999.

[18] L. Bossi, C.Rottenbacher, G.Mimmi, L.Magni, **"Multivariable Predictive Control for Vibrating Structures: An application",** *Control Engineering Practice 19*, pp. 1087–1098, 2011.

[19] A. Jadlovská, N. Kabakov, J. Sarnovský, **"Predictive Control Design Based on Neural Model of a Non-linear System",** Journal of *Applied Sciences, Acta Polytechnica Hungarica*, Vol. 5, No. 4, pp. 93-108, 2008.

[20] H. Khouidmi, A. Massoum, **"Neural Networks Generalized Predictive Speed Controller for Vector Controlled Double Stator Induction Motor",** *Majlesi Journal of Mechatronic Systems*, Vol. 03, No. 2, pp. 13-18, 2014.

[21] A. Jadlovská, Š. Jajčišin, **"Predictive Control Algorithms Verification on the Laboratory Helicopter Model",** *Journal of Applied Sciences, Acta Polytechnica Hungarica*, Vol. 9, No. 4, pp. 221-245, 2012.

[22] A.F. Syed, Ch.A. Fahad, H. Desa, A T. Hussain, **"Model Predictive Controller-based, Single Phase Pulse Width Modulation (PWM) Inverter for UPS Systems",** *Journal of Applied Sciences, Acta Polytechnica Hungarica*, Vol. 11, No. 6, pp. 23-38, 2014.